MODELING THE FAILURE STRENGTH OF DEBONDED COMPOSITE SANDWICH STRUCTURE

Yi-Hsin Nieh[a], Yen-Kun Lai[a], Jia-Lin Tsai[a*]

[a]*Department of Mechanical Engineering, National Chiao Tung University, Hsinchu, Taiwan, 300*
**jialin@mail.nctu.edu.tw*

Keywords: debonded composite sandwich structure, failure analysis, finite element analysis

Abstract
The research aims to investigate the failure behaviors of the composite sandwich structures with debond defect subjected to compression loading. Experimental results revealed that the sandwich structures with either thick face-sheet or short debonded length exhibit higher failure strength. Moreover, when the debonded length is short, the failure is dominated by global buckling followed by core failure. Nevertheless, when the debonded length is long, the failure mechanism becomes the local buckling followed by the crack extension from the debond defect tip. The nonlinear finite element simulation was performed on the sandwich samples for the failure analysis. It was found that when the failure is dominated by the global buckling, the strength can be characterized using the maximum principal strain criterion. On the other hand, when the failure mode is local buckling, the failure strength can be predicted using the damage zone method.

1. Introduction

With the high bending rigidity and light weight, the composite sandwich structures have been extensively utilized in aerospace, vehicle and wind turbine, etc. The sandwich structures are composited of high stiff composite face sheets and the low density form core. The form core is sandwiched between two face sheets and the laminate is bonded together using adhesive to form the sandwich structure. The purpose of the face sheet is to withstand the axial loading; nevertheless the function of the form core is to augment the bending rigidity of the structure by enlarging the moment of inertia of the cross section. During the manufacturing process or the engineering operation, possibly there is debond defect generated between the face sheet and form core such that the performances of the sandwich structures are significantly influenced. [1-3]. Thus, it is required to understand the behavior of the debonded sandwich structures for the damage tolerance as well as the engineering application with safety. In this study, the debonded sandwich specimens containing various debonded lengths and different face sheet thickness were manufactured and then tested in compression. The failure loads as well as the failure mechanisms were observed during the loading process. Successively, the nonlinear finite element analysis was carried out to simulate the failure behaviors of the debonded sandwich structures. Both experimental data and simulation results were compared and discussed with each other.

2. Experiments

The composite sandwich samples contain the form core and the composite face sheet. The Polymethacrylimide (PMI) form was obtained from ROHACELL® (51WF), and the face sheet is graphite/epoxy composites with two different layup sequences, i.e., $[(0/90)_2]_S$ and $[(0/90)_3]_S$. The composite face sheets and form core were adhered together using the FM73 adhesive film. A thin layer of Teflon was inserted between the face sheet and the form core during the fabrication for the artificial generation of an initial debond defect. In this study, the debonded lengths (L_d) were respectively designated as 10mm, 30mm, 50mm, 60mm and 70mm. The dimension of the sandwich specimens are shown in Figure 1. In addition, two gages (gage A in on the debonded face, gage B is on the bonded face) were mounted on the specimen to measure the deformation during the compressive loading. The compression tests were conducted on the MTS machine with the displacement rate of 0.002mm/s, from which the load strain curves were obtained. Basically for each case, at least three samples were tested. The experimental setup for the sandwich compression tests is shown in Figure 2.

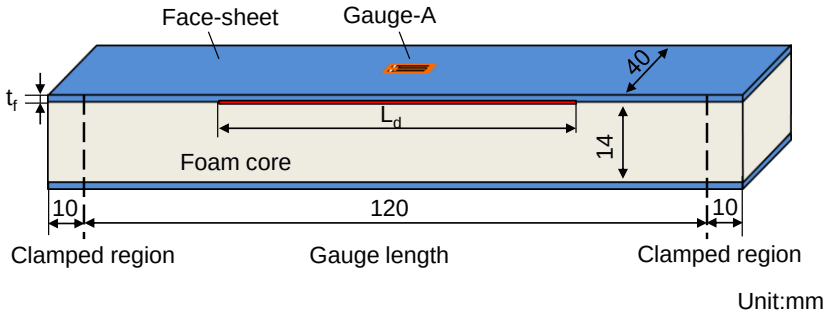

Figure 1. Dimension of the debonded sandwich specimens

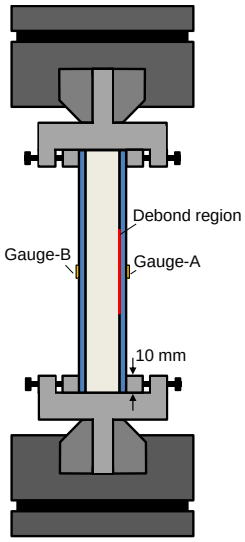

Figure 2. Schemetic of experimental setup for the compression tests of the debonded sandwich samples

The load deflection curves measured from the strain gages for the sandwich sample with 50mm debonded length is shown in Figure 3. It can be seen that the debond region (gage A) is in compression initially and then become in tension. The transition from the compression to the tension indicates the occurring of local buckling in the debond region as shown in figure 4(a). Subsequently, the crack extends from the debond tip yielding the sudden failure as shown in Figure 4(b). The compression loading corresponding to the maximum compressive

strain in the debond region was regarded as the buckling load. Furthermore, the maximum compressive loading during the tests was considered as the failure load of the specimen. It can be seen that after the local buckling occurs, the specimen can still sustain more loading until the ultimate loading is achieved. Apparently, the face sheet and form core separation caused by the local buckling is the main failure mechanism. Figure 5 is the load deflection curves for the samples with 10mm debonded length. In such case, the main failure mode is global buckling followed by the core failure as shown in Figure 6. It can be seen that the crack appears within the form core which is orientated around 45^{o} to the loading direction. The experimental results of the sandwich specimens with different debonded length and face sheet thickness are summarized in Table 1. For the sandwich specimens with $[(0/90)_2]_s$ face sheets and debonded length is less than 10 mm or the sandwich specimens with $[(0/90)_3]_s$ face sheets and debonded length is less than 30 mm, the main failure mode is global bucking together with the core failure. In such failure mode, the specimens demonstrate higher buckling and failure load than those which fails associated with local buckling. In other words, the sandwich structures with less debonded length and thicker face sheet exhibit high failure strength. Moreover, it was found that once the failure is dominated by the core failure, the buckling load and the failure load are quite close and the corresponding values are not influenced by the debonded length. Thus, for the $[(0/90)_2]_s$ face sheet case, the failure load of the sandwich specimens are around 18 MPa, on the other hand, for the $[(0/90)_3]_S$ face sheet cases, the corresponding values are around 21 MPa. It should be caution that when the global buckling occurs, the sandwich specimens almost cannot endure more loading. Nevertheless, when the debonded length is long, the failure mechanism apparently becomes the local buckling followed by the crack extension from the debond defect tip. In such failure mode, the failure load is much higher the buckling load, which indicates that the specimens can still sustain more loading after the local buckling takes place. Furthermore, both failure load and buckling load are quite relied on the debonded length. When the debonded length inceases, the corresponding values are declined. With regard to the face sheet thickness, it is indicated that in terms of the same debonded length, the sandwich with thicker face sheet always exhibits higher buckling and failure loading, no matter what kind of failure mode is dominant.

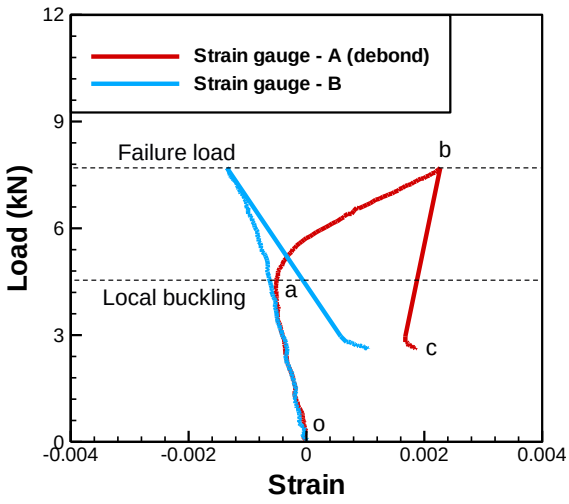

Figure 3. Load deflection curves measured from the strain gages for $[(0/90)_2]_S$ sandwich sample with 50 mm debonded length

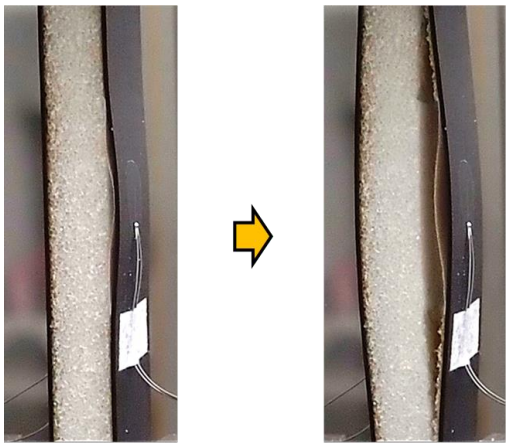

Figure 4. Fracture behaviors for $[(0/90)_2]_S$ sandwich sample with 50 mm debonded length ((a) local buckling, (b) face sheet and core separation induced failure)

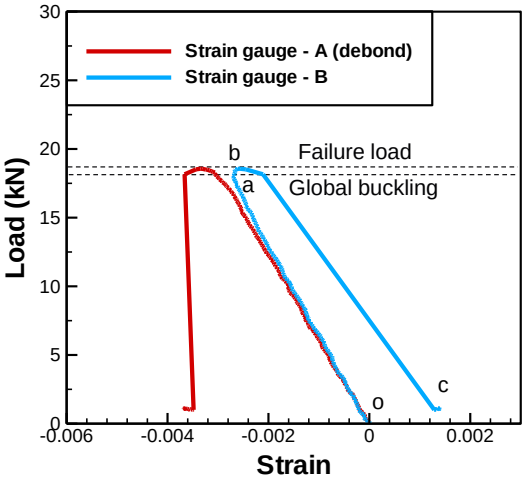

Figure 5. Loading curves for the $[(0/90)_2]_S$ specimens with debonded length of 10 mm

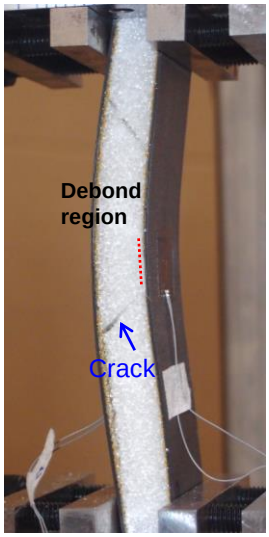

Figure 6. Photos of the failed $[(0/90)_2]_S$ specimens with debonded length of 10 mm

Face-sheet laminate	Debonded length(mm)	Buckling load (kN)	Failure load(kN)	Failure mode
$[(0/90)_2]_S$	0	18.0 ± 0.2	18.3 ± 0.2	Core failure
	10	17.7 ± 1.9	18.3 ± 1.6	
	30	10.8 ± 0.4	12.7 ± 0.7	Face-sheet and core separate
	50	4.6 ± 0.8	8.0 ± 1.7	
	60	3.6 ± 0.2	8.0 ± 0.6	
	70	2.9 ± 0.6	7.7 ± 0.9	
$[(0/90)_3]_S$	0	21.6 ± 0.2	22.4 ± 0.2	Core failure
	10	21.4 ± 0.7	22.3 ± 0.5	
	30	20.5 ± 0.9	21.7 ± 0.2	
	50	13.7 ± 0.4	16.2 ± 0.5	Face-sheet and core separate
	60	9.6 ± 0.8	13.8 ± 0.4	
	70	8.0 ± 0.7	11.7 ± 0.5	

Table 1. Experimental results of $[(0/90)_2]_S$ and $[(0/90)_3]_S$ composite sandwich specimens

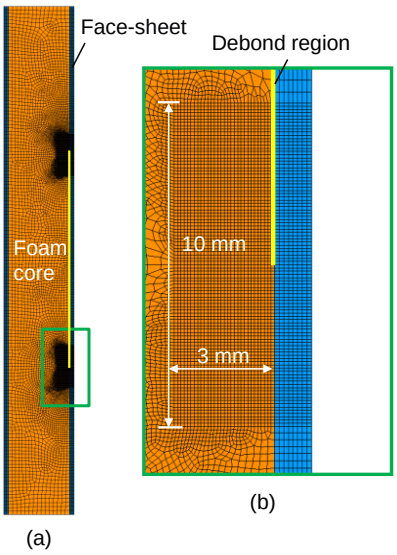

Figure 7. FEM model for the debonded composite sandwich structure ((A) the whole model,(b) the local mesh near the debond tip)

Young's modulus			Poisson's ratio			Shear modulus		
E_{11} (GPa)	E_{22} (GPa)	E_{33} (GPa)	ν_{12}	ν_{23}	ν_{13}	G_{12} (GPa)	G_{23} (GPa)	G_{13} (GPa)
145.9	9.7	9.7	0.3	0.3	0.3	5.6	5.6	5.6

Table 2. Material properties of fiber composites

3. Finite element analysis

In order to characterize the failure behaviors of the debonded sandwich specimens, the nonlinear finite element analysis were carried out using the commercial code ANSYS. Figure 7 illustrates the 2D FEM meshes in which the sandwich specimen was modeled using plane 183 element. Furthermore, in the debond region, the contact elements (CONTA 172 and TARGE 169) were established on the interface to prevent the penetration taking place. It is noted that there is stress singularity near the debond defect tip and thus the fine mesh as

shown in Figure 7(b) was generated. The material properties of the graphite/epoxy composites are shown in Table 2. In addition, the material properties for the form core can be found elsewhere in the manufacturing company website [4]. The FEM analysis basically contains two steps. In the first step, the linear analysis was utilized to obtain the first buckling mode shape. Afterwards, the buckling model with small perturbation was introduced in the nonlinear FEM analysis where the nonlinear large deformation was taken into account [5]. The extent of the small perturbation was modified such that the simulated load deflection curve is in good agreement with the experimental one. From the nonlinear FEM simulation, the buckling load corresponding to the maximum tensile strain in the debond region were determined and the results were compared with experimental data as shown in Table 3. It seems that the FEM results are quite close to the experimental results.

Face-sheet laminate	Debonded length (mm)	Buckling load (kN)	
		Analysis	Exp.
$[(0/90)_2]_S$	0	17.6	18.0 ± 0.2
	10	17.4	17.7 ± 1.9
	30	10.2	10.8 ± 0.4
	50	5.1	4.6 ± 0.8
	60	3.9	3.6 ± 0.2
	70	3.2	2.9 ± 0.6
$[(0/90)_3]_S$	0	22.7	21.6 ± 0.2
	10	22.7	21.4 ± 0.7
	30	19.9	20.5 ± 0.9
	50	13.6	13.7 ± 0.4
	60	10.0	9.6 ± 0.8
	70	8.3	8.0 ± 0.7

Table 3. Comparison of buckling loads obtained from simulation and experiments

Face-sheet laminate	Debonded length (mm)	Failure load (kN)	
		Analysis	Exp.
$[(0/90)_2]_S$	0	17.6	18.3 ± 0.2
	10	17.6	18.3 ± 1.6
	30	13.0	12.7 ± 0.7
	50	8.0	8.0 ± 1.7
	60	6.9	8.0 ± 0.6
	70	6.4	7.7 ± 0.9
$[(0/90)_3]_S$	0	23.7	22.4 ± 0.2
	10	23.6	22.3 ± 0.5
	10	23.7	22.3 ± 0.5
	30	21.6	21.7 ± 0.2
	50	16.3	16.2 ± 0.5
	60	13.6	13.8 ± 0.4
	70	12.0	11.7 ± 0.5

Table 4. Comparison of failure loads obtained from simulation and experiments

The failure behaviors of the sandwich specimens were characterized using either the damage zone model [6] or the maximum principal strain criterion. For the specimen with form core failure, the corresponding failure loads were predicted using the maximum principal strain

criterion. This is because the form core is a brittle material and easily to be failure under tensile deformation. On the other hand, when the failure is dominated by the crack extended from the debond tip, the damage zone model was adopted for the strength prediction. Basically, the damage zone model can effectively avoid the stress singularity near the debond tip by introducing the area failure concept rather than the point failure concept for failure prediction. The comparison of the FEM results with the experimental data is shown in Table 4. It reveals that the tendency of both results agree well, although there is difference of 10% found in some samples.

4. Conclusions

The failure behaviors of the composite sandwich structures with debond defect subjected to compression loading was examined experimentally and numerically. Experimental results depict that the sandwich structures with either thick face-sheet or short debonded length exhibit higher failure strength. When the debonded length is short, the failure is dominated by global buckling followed by core failure, and the failure load is close to the buckling load Nevertheless, when the debonded length is long, the failure mechanism becomes the local buckling followed by the crack extension from the debond defect tip. In this failure mode, the failure load is higher than the buckling load. The nonlinear finite element simulation was performed on the sandwich samples for the failure analysis. It was found that when the failure is dominated by the core failure, the strength can be characterized using the maximum principal strain criterion. On the other hand, when the failure mode is governed by local buckling, the failure strength can be predicted using the damage zone method. Both experimental results and simulations are in an agreement with each other.

References

[1] V. Vadakke and L. A. Carlsson. "Experimental investigation of compression failure of sandwich specimens with face/core debond," *Composites Part B: Engineering*, vol. 35: 583-590, 2004.
[2] J. L. Avery III and B. V. Sankar. "Compressive failure of sandwich beams with debonded face-sheets," *Journal of composite materials*, vol. 34: 1176-1199, 2000.
[3] F. Avilés and L. A. Carlsson. "Experimental study of debonded sandwich panels under compressive loading," *Journal of Sandwich Structures and Materials*, vol. 8: 7-31, 2006.
[4] Website:http://www.rohacell.com/product/rohacell/en/products-services/rohacell-wf/pages/default.aspx.
[5] B. V. Sankar and M. Narayanan. "Finite element analysis of debonded sandwich beams under axial compression," *Journal of Sandwich Structures and Materials*, vol. 3: 197-219, 2001.
[6] A. Sheppard, D. Kelly, and L. Tong. "A damage zone model for the failure analysis of adhesively bonded joints," *International journal of adhesion and adhesives*, vol. 18: 385-400, 1998.